

Entanglement, fidelity, and topological entropy in a quantum phase transition to topological order

A. Hamma,¹ W. Zhang,² S. Haas,² and D. A. Lidar^{1,2,3}

¹*Department of Chemistry, Center for Quantum Information Science & Technology,
University of Southern California, Los Angeles, California 90089, USA*

²*Department of Physics and Astronomy, Center for Quantum Information Science & Technology,
University of Southern California, Los Angeles, California 90089, USA*

³*Department of Electrical Engineering, Center for Quantum Information Science & Technology,
University of Southern California, Los Angeles, California 90089, USA*

(Received 7 March 2008; published 9 April 2008)

We present a numerical study of a quantum phase transition from a spin-polarized to a topologically ordered phase in a system of spin-1/2 particles on a torus. We demonstrate that this non-symmetry-breaking topological quantum phase transition (TOQPT) is of second order. The transition is analyzed via the ground state energy and fidelity, block entanglement, Wilson loops, and the recently proposed topological entropy. Only the topological entropy distinguishes the TOQPT from a standard QPT, and remarkably, does so already for small system sizes. Thus the topological entropy serves as a proper order parameter. We demonstrate that our conclusions are robust under the addition of random perturbations, not only in the topological phase, but also in the spin-polarized phase and even at the critical point.

DOI: [10.1103/PhysRevB.77.155111](https://doi.org/10.1103/PhysRevB.77.155111)

PACS number(s): 03.65.Ud, 03.67.Mn, 05.50.+g

I. INTRODUCTION

A quantum phase transition (QPT) occurs when the order parameter of a quantum system becomes discontinuous or singular.¹ This is associated with a drastic change of the ground state wave function. Unlike classical phase transitions, QPTs occur at $T=0$ and thus are not driven by thermal fluctuations. Instead, quantum fluctuations are capable of changing the internal order of a system and cause the transition. When a quantum Hamiltonian $H(\lambda)$, which depends smoothly on external parameters λ , approaches a quantum critical point λ_c from a gapped phase, the gap Δ above the ground state closes, and the critical system has gapless excitations. This corresponds to a continuous, second order QPT.

Here, we consider a QPT from a spin-polarized to a topologically ordered phase: a topological quantum phase transition (TOQPT). The internal order that characterizes topologically ordered phases cannot be explained by the standard Ginzburg-Landau theory of symmetry breaking and local order parameters. Instead, it requires the notion of *topological order* (TO).² TO manifests itself in a ground state degeneracy, which depends on the topology of the physical system, and it is robust against arbitrary local perturbations.³ This robustness is at the root of topological quantum computation, i.e., the ground state degeneracy can be used as a robust memory, and the topological interactions among the quasiparticles can be used to construct robust logic gates.^{4,5} On the other hand, to what extent a TOQPT is affected by perturbations is a problem that has only very recently been addressed,^{6,7} and is a focus of this work. Moreover, the classification of TO is still an open question. Ground state degeneracy, quasiparticle statistics, and edge states, all measure and detect TO but do not suffice to give a full description. Tools from quantum information theory, specifically entanglement^{8,9} and the ground state fidelity,¹⁰ have recently been widely exploited to characterize QPTs. To date, all the

QPTs studied with these tools have been of the usual symmetry-breaking type. Here we apply them to the transition from a spin-polarized phase to a TO phase, and find that they are universal in the sense that they detect this transition. However, these tools do not suffice to distinguish a symmetry-breaking QPT from a TOQPT. Recently, the new concept of “topological entropy” S_{top} was introduced.¹¹ The topological entropy vanishes in the thermodynamic limit for a normal state, whereas $S_{\text{top}} \neq 0$ for a TO state. Therefore, S_{top} can serve as an order parameter. Moreover, TO is not only a property of infinite systems, an important question that was left open in Ref. 11 is the behavior of S_{top} for finite systems. Here we shed light on this question by presenting finite-system calculations of S_{top} . We report that S_{top} changes abruptly at the critical point of a phase transition between phases with and without TO, even for very small systems. It is thus an excellent discriminator between the absence and presence of TO, and moreover, S_{top} is capable of detecting a TOQPT.

Specifically, we present an exact time-dependent numerical study of a TOQPT, introduced in Ref. 6, from a spin-polarized phase to a TO phase, for both the ideal model and the model in the presence of an external perturbation. Our results are the following: (i) standard QPT detectors (derivative of the ground state energy,¹ entanglement of a subsystem with the remainder of the lattice,^{8,9} ground state fidelity¹⁰), are all singular at the critical point of the TOQPT, thus confirming that this is indeed a QPT. Ground state fidelity and block entanglement are thus capable of dealing also with non-symmetry-breaking QPTs. (ii) S_{top} detects the TOQPT in a very sharp manner already for small system sizes. It also detects TO better than other nonlocal order parameters, in particular, the expectation value of Wilson loops. It is therefore appropriate for the detection and characterization of TOQPTs and for studying TO. These results complement and strengthen the conclusions of Ref. 11. (iii) Adiabatic evolu-

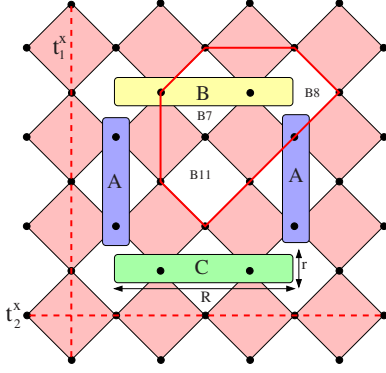


FIG. 1. (Color online) A square lattice with 32 spins. The spin degrees of freedom are placed on the vertices. The red dashed lines r_1^x, r_2^x are the incontractible loops around the torus. The product $B7 \times B8 \times B11$ denotes the loop operator drawn in red. All the spins on the vertices crossed by a loop are flipped. The region $A \cup B \cup C$ is a ring containing eight spins, used in computing S_{top} . For the lattice of 32 spins, the ring has diameter $R=2$ and width $r=1$.

tion can initialize topological quantum memory faithfully: even in the presence of perturbations the coupling to other topological sectors and excited states is negligible. (iv) This robustness extends to the entire topological phase, and even to the critical point itself. Perturbations do not affect the nature of the TOQPT either.

II. PRELIMINARIES

Consider a square lattice L with periodic boundary conditions (torus) and with n spin-1/2 degrees of freedom occupying its vertices. The Hilbert space is given by $\mathcal{H} = \text{span}\{|0\rangle, |1\rangle\}^{\otimes n}$, where $|0\rangle$ and $|1\rangle$ are the \pm eigenvectors of the Pauli σ^z matrix. As shown in Fig. 1, the n plaquettes can be partitioned into two sublattices, denoted by different colors. Following Kitaev,⁴ we associate with every white plaquette p an operator $B_p \equiv \prod_{j \in \partial p} \sigma_j^x$ that flips all spins along the boundary of p . A “closed string operator” is a product of plaquette operators B_p that flips all spins around a loop (or around a loop net). The “group of closed strings” \bar{X} is the group of products of plaquettes B_p . Similarly, with every pink plaquette s , we associate an operator $A_s \equiv \prod_{j \in s} \sigma_j^z$ which counts if there is an even or odd number of flipped spins around the plaquette s . Kitaev’s toric code Hamiltonian⁴ is then given by $H_{U,g} = -U \sum_s A_s - g \sum_p B_p \equiv H_U + H_g$, which realizes a Z_2 lattice gauge theory in the limit $U \rightarrow \infty$. The ground state is an equal superposition of all closed strings (loops) acting on the spin-polarized state $|\text{vac}\rangle \equiv |0\rangle_1 \otimes \dots \otimes |0\rangle_n$ —it is in a *string-condensed* phase. The ground state manifold is given by $\mathcal{L} = \text{span}\{|\bar{X}|^{-1/2} (r_1^x)^i (r_2^x)^j \sum_{x \in \bar{X}} x |\text{vac}\rangle; i, j \in \{0, 1\}\}$, which is fourfold degenerate.¹² The $r_{1,2}^x$ s flip all the spins along an incontractible loop around the torus (see Fig. 1), taking a vector in \mathcal{L} to an orthogonal one in the same manifold because they commute with $H_{U,g}$. On a lattice on a Riemann surface of genus g , there are $2g$ incontractible loops $\{r_j^x\}_{j=1}^{2g}$, and therefore \mathcal{L} is 2^{2g} -fold degenerate^{4,14} (for a torus $g=1$).

Model and the QPT. Now consider the following time-

dependent Hamiltonian, introduced in Ref. 6 as a model for a TOQPT:

$$H_0(\tau) = H_U + \tau H_g + (1 - \tau) H_\xi, \quad (1)$$

where $H_\xi \equiv -\xi \sum_{r=1}^n \sigma_r^z$, $\tau = t/T \in [0, 1]$, and T is the total time. The nondegenerate ground state of $H(0) = H_U + H_\xi$ is the spin-polarized state $|\text{vac}\rangle$, which is the vacuum of the strings. The term $(1 - \tau) H_\xi$ acts as a tension for the strings, whereas τH_g causes the strings to fluctuate. As τ increases, the string fluctuations increase while the loop tension decreases. For a critical value of $\lambda \equiv \tau g / (1 - \tau) \xi$, and in the thermodynamic limit, a continuous QPT occurs to a TO phase of string condensation. This QPT is not symmetry breaking, i.e., is a TOQPT. As argued in Ref. 6, provided $T \gg 1/\Delta_{\text{min}}$ (the minimum gap, as a function of τ , between the ground state and the first excited state) evolution according to $H(\tau)$ is an adiabatic preparation mechanism of a TO state: one of the 2^{2g} degenerate ground states of Kitaev’s toric code model.⁴ Reference 6 showed that $\Delta_{\text{min}} \sim 1/\sqrt{n}$. $H(\tau)$ can be mapped onto an Ising model in a transverse field, which is known to have a second order QPT⁶ (see also Ref. 7). However, in this work we do not resort to such a mapping, because it is nonlocal and does not preserve entanglement measures. Instead, we numerically study $H(\tau)$ for $\tau \in [0, 1]$ in $\Delta\tau=0.01$ increments on lattices Ln with $n=\{8, 18, 32\}$ spins, and set $U=100$, $\xi=g=1$. The computational methods used here are (i) the Housholder algorithm¹⁵ for the full diagonalization (all eigenstates) of $L8$, and (ii) a modified Lanczos method¹⁶ to obtain the low-energy sectors of $L18$ and $L32$. We observe that for all $\tau \in [0, 1]$ the ground state comprises only closed strings. Since this is the case for every finite system size, and in order to reduce computation cost, we diagonalize $L32$ only in the relevant symmetry subspaces, defined by the constraint $A_s |\psi\rangle \equiv \prod_{j \in s} \sigma_j^z |\psi\rangle = |\psi\rangle$, $\forall s$.

III. PERTURBED MODEL

To test the robustness of the TOQPT, we also studied the perturbed model given by

$$H(\tau) = H_0(\tau) + V \equiv H_0(\tau) + \sum_{j=1}^n [h^x(j) \sigma_j^x + h^z(j) \sigma_j^z]. \quad (2)$$

The perturbation V is random with $h^z(j)$ and $h^x(j)$ uniformly distributed in $[-0.2, 0.2]$ and $[-P, P]$, respectively, with the magnitude P variable in our calculations below. We carried out calculations for $L8$ (time-dependent) and $L18$ (ground state only). These were averaged over random realizations of V , and included the full Hilbert space as V disrupts the symmetry $A_s |\psi\rangle = |\psi\rangle$. The z component of the perturbation is expected to have a small effect as it only slightly modifies the term H_ξ for $\tau < \tau_c$, while for $\tau > \tau_c$ TO dominates and tension effects are suppressed. Our calculations confirmed this, and hence Figs. 2–7 show the results for $h^z(j) \equiv 0$.

IV. ADIABATIC EVOLUTION

We numerically simulated the time evolution from the fully polarized state at $\tau=0$ to the string-condensed phase at

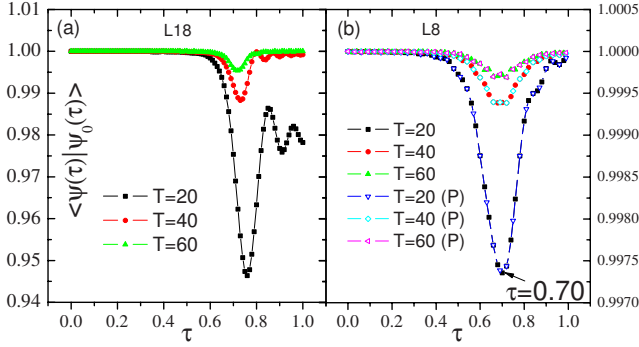


FIG. 2. (Color online) Fidelity between the time-dependent solution of the Schrödinger equation and the adiabatic state, for different values of the total evolution time: $T=20,40,60$. (a) The unperturbed model for $L18$. The evolution is adiabatic for $T=60$. Note that the drop in adiabaticity is a precursor of the QPT. (b) $L8$: fidelity in both the ideal and perturbed ($P=1$) cases. The perturbed model is indistinguishable from the ideal one.

$\tau=1$. The possibility of preparation of topological order via such evolution has been studied theoretically in Ref. 6. A crucial point is to show that the adiabatic time depends on the minimum gap that marks the phase transition (and that is polynomially small in the number of spins), and not on the exponentially small splitting of the ground state in the topological phase. To this end, one must show that transitions to other topological sectors are forbidden and protected by topology.⁶ The initial wave function is the exactly known ground state of $H(\tau=0)$. This state is then used as the seed to compute the ground state of $H(\Delta\tau)$. After iteration, this state

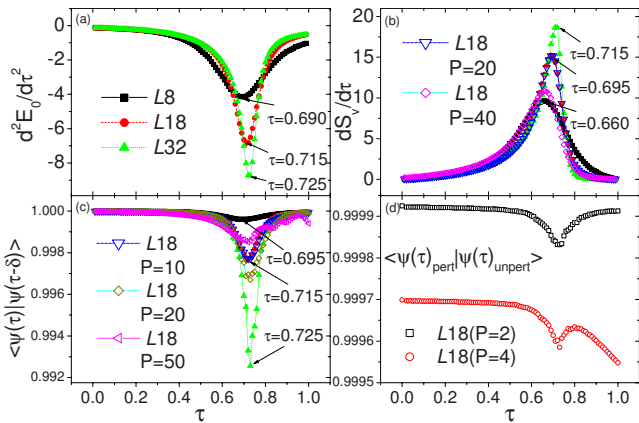


FIG. 3. (Color online) QPT detectors for $L8, L18, L32$, for the unperturbed and perturbed model. All graphs show strong resilience of the model and its QPT against perturbations: (a) Second derivative of $E(\tau)$, diverging for $\tau_c \sim 0.7$. The QPT is thus second order. (b) Derivative of the von Neumann entropy, measuring the entanglement of a plaquette with the rest of the lattice. Its divergence at criticality also signals a second order QPT. The perturbation has no effect for $P=20$ (triangles indistinguishable from circles) but is visible for $P=40$. (c) Ground state fidelity $\mathcal{F}(\tau)$: the fidelity drop at the critical point signals a QPT, associated with a drastic change in the properties of the ground state. (d) Overlap between the perturbed and the ideal ground state. The clearly visible susceptibility to the perturbation at the critical point also signals the QPT.

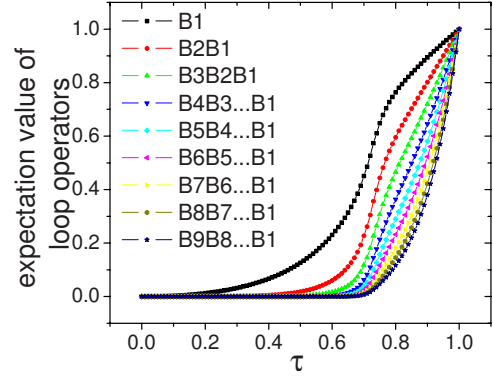


FIG. 4. (Color online) Expectation value of Wilson loop operators of increasing size for $L32$. The expectation value of the loop operators starts to increase at τ_c , more steeply so for the largest loops, indicating that this observable can be used to detect the TOQPT for large systems.

is in turn used as the seed for $H(2\Delta\tau)$, etc. We can estimate to what extent the evolution is adiabatic by numerically solving, for $L18$, the time-dependent Schrödinger equation $H\psi(\tau) = i\dot{\psi}(\tau)$ for different values of the total evolution time T . This is shown in Fig. 2(a), where we plot the fidelity between the time-evolved wave function $\psi(\tau)$ and the instantaneous ground state: $\mathcal{F}_{\text{ad}} = |\langle \psi(\tau) | \psi_0(\tau) \rangle|$. Moreover, we compute \mathcal{F}_{ad} also for the perturbed model, but the largest lattice for which we can do this is $L8$. Figure 2(b) shows clearly that for $P=1$ the perturbation does not change the time-evolved state. Significant effects start at $P=2$ (not shown). We also find that the overlap between the evolved wave function $\psi(\tau)$ and the other sectors $(r_1^i)^i (r_2^j)^j | \psi_0(\tau) \rangle$ is of order $\sim 10^{-3}$ for every $(i,j) \neq (0,0)$ and value of T tested. This is numerical evidence for the argument that time evolution will always keep the instantaneous eigenstate within a topological sector, even in the presence of perturbations.⁶ Thus the relevant gap for adiabatic evolution is that to the other closed string excited states, which implies that the evolution into the TO sector can be used to prepare a topological quantum memory.⁶ Henceforth we work only in the sector $(i=0, j=0)$, into which the system is initialized as the unique ground state of $H(\tau=0)$.

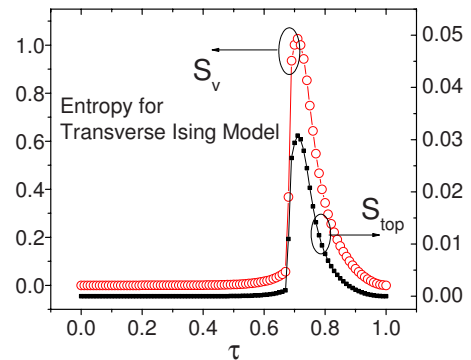


FIG. 5. (Color online) von Neumann entropy for a plaquette of spins and S_{top} for $L32$ with an Ising Hamiltonian in a transverse field. Note the different vertical scales. For a system without topological order, S_{top} is always ~ 0 (the small bump is a finite-size effect).

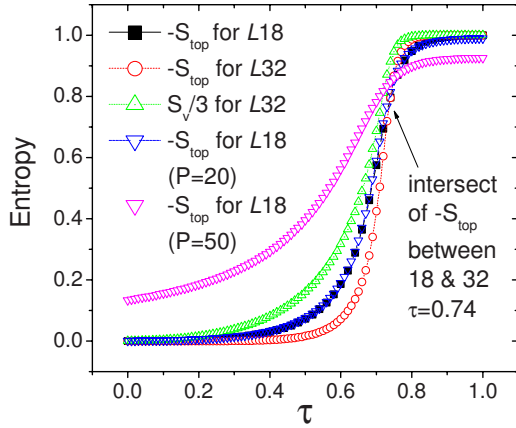


FIG. 6. (Color online) S_{top} for L18 and L32, and von Neumann entropy for L32, for the ideal and perturbed model. S_v assumes the value $l-1=3$ in the entire TO phase, where $l-1$ is the exact value of S_v for the pure Kitaev model ($\tau=1$) and $l=4$ is the length of the border of a plaquette. S_{top} is zero in the spin-polarized phase and quickly reaches unity in the TO phase. Also the topological character of the QPT and of the phases is resilient to perturbations.

V. DETECTING THE QPT WITH STANDARD MEASURES

To check that the transition from magnetic order to TO is indeed a QPT, we first computed the energy per particle of the ground state for L8, L18, L32, and its second derivative. As seen in Fig. 3(a), the latter develops a singularity as system size increases, signaling a second order QPT with a critical point at $\tau \sim 0.71$, corresponding to a ratio $\xi/g \sim 0.41$. This is in good agreement with the analytical study,¹⁸ which obtained (in the thermodynamic limit) $\xi/g \sim 0.44$, even if this model is only asymptotically equivalent to the toric code in a magnetic field, in the small field limit. On the other hand, Ref. 7 found $\xi/g \sim 0.33$, using a mapping to the classical 3D Ising model. In Fig. 3(b) we show the block entanglement between four spins in a small loop (B_{11} , Fig. 1) and the rest of the lattice, as measured by the von Neumann entropy. In agreement with the general theory,⁹ the derivative of the entanglement diverges at the critical point for a second order QPT.

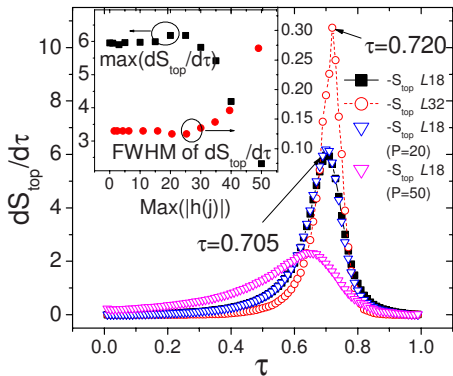


FIG. 7. (Color online) First derivative of S_{top} for L18 and L32, for the ideal and perturbed model, diverging at τ_c thus signaling the TOQPT; (inset) derivative and full width at half maximum of S_{top} at τ_c as a function of perturbation strength P . S_{top} remains robust up to $P \sim 25$.

A new interesting alternative characterization of QPTs can be given in terms of the scaling in the fidelity $\mathcal{F}_{\Delta\tau}(\tau) = |\langle \psi(\tau) | \psi(\tau - \Delta\tau) \rangle|$ between two different ground states.¹⁰ At a quantum phase transition, the fidelity should scale to zero superextensively. Previous work^{10,20} has shown that the fidelity criterion is valid for generic symmetry-breaking second order QPTs. Nevertheless, the fidelity criterion is not strictly local, so one would like to know whether it detects the QPT to a topologically ordered state. The results are shown in Fig. 3(c). The fidelity drop criterion indeed also detects the QPT. Figures 3(a)–3(c) also show the result for the perturbed model.

By looking at the behavior of the transition in the presence of perturbations, we can safely conclude that the QPT is unaffected by the perturbation for $P \leq 10$, namely, the value of τ_c and the magnitude of the fidelity drop remain unchanged. In Fig. 3(d), we plot the overlap between the perturbed and unperturbed ground state. The drop in this quantity also signals the QPT, showing that the system is most sensitive to perturbations at the critical point (see also Ref. 19). Interestingly, in contrast to the robustness of the entanglement and $\mathcal{F}_{\Delta\tau}(\tau)$, the perturbed and unperturbed ground states differ significantly already for $P > 2$. The results in Fig. 3 thus allow us to infer unambiguously that there is indeed a second order QPT in the adiabatic dynamics generated by $H(\tau)$. However, none of the quantities shown in Fig. 3 is explicitly designed to detect topological features, and hence these quantities are incapable of distinguishing between a symmetry-breaking QPT and a TOQPT.

VI. CHARACTERIZING THE TOPOLOGICAL PHASE

The spin-polarized regime for $\tau < \tau_c$ is characterized by a finite magnetization. On the other hand, the topologically ordered phase $\tau > \tau_c$ does not admit a local order parameter.¹⁷ The topologically ordered phase is a string-condensed phase and an effective Z_2 local gauge theory and thus the observables must be gauge invariant quantities. These quantities are the Wilson loops. In this theory, we make a Wilson loop $W^{x(z)}[\gamma]$ of the $x(z)$ type by drawing a closed string γ on the lattice, and operating with $\sigma^x(\sigma^z)$ on all the spins encountered by the loop. In the polarized phase, the tension is high and it is difficult to create large loops. The expectation value of loops decays with the area enclosed by the loop. In the topologically ordered phase, large loops are less costly and their expectation value only decays at most with the perimeter of the loop. The phase transition is of the confinement or deconfinement type. We can write any (contractible) Wilson loop as the product of some plaquette operator: $W^{x(z)}[\gamma] = \prod_{k \in \gamma} B_k$. In particular, at the point $\tau=1$ when the model is the exact toric code, the expectation value of Wilson loops is $\langle W^{x(z)}[\gamma] \rangle = 1$ for every loop γ , independently of its size. Of course, large loops are highly nonlocal observables. We have computed the expectation value of Wilson loop operators of increasing size as a function of τ . As Fig. 4 shows, the expectation values of large loops vanish in the spin-polarized phase, and increase exponentially in the TO phase. However, in the limit of infinite length, Wilson loops are not observables of the pure gauge theory²¹ and cannot be measured.

Nevertheless, topological order reveals itself in the way the ground state is entangled. If we compute the von Neumann entropy for a region with perimeter L , the entanglement entropy will be $S=L-1$ in the topological phase—see Fig. 6. The spin-polarized phase is not entangled. We see that there is a finite correction of -1 to the boundary law for the entanglement, which is due to the presence of topological order.^{13,14} Therefore we can consider as an alternative non-local order parameter the *topological entropy*:¹¹

$$S_{\text{top}}^{(R,r)} = S_{(A \cup B \cup C)} - S_{(A \cup C)} - S_{(A \cup B)} + S_A, \quad (3)$$

where S_σ are the entanglement entropies associated with four cuts $\sigma = \{A \cup B \cup C, A \cup C, A \cup B, A\}$, as depicted in Fig. 1. We computed $S_{\text{top}}(\tau)$ in the instantaneous ground state $|\psi(\tau)\rangle$ for $L18$ and $L32$ ($L8$ is too small) in the ideal model and for $L18$ in the perturbed model—see Figs. 5–7. In the spin-polarized phase, even for finite systems, $S_{\text{top}}=0$ and it becomes different from zero only in the vicinity of the critical point, after which it rapidly reaches 1 (as predicted in the thermodynamic limit in Ref. 11). To test whether S_{top} can discriminate between symmetry-breaking QPTs and TOQPTs, we show in Fig. 5 the behavior of block entanglement and S_{top} for a quantum *Ising model* in 2D. This model admits a QPT between a paramagnetic and magnetically ordered phase, which is symmetry breaking. Block entanglement detects the critical point sharply, while S_{top} does not (note the different scales on the left and right vertical axes). The small nonzero value of S_{top} is a finite-size effect.

The block entropy in Fig. 6 shows that the state is already rather entangled in the spin-polarized region, whereas S_{top} is almost zero before the transition to TO occurs. Note that the block entanglement at the critical point is bounded from above by the final-state entanglement ($\tau=1$), which obeys the area law. This is an example of the fact that in 2D, critical systems do not need to violate the area law as in 1D. The useful feature of S_{top} is not only that it can be used in order to locate the critical point (Fig. 7), but also that it allows one to understand the type of QPT (symmetry-breaking or TO). Remarkably, Figs. 5 and 7 show that S_{top} has these properties already for finite and very small systems. The accuracy of the finite-size S_{top} at the limit points $\tau=0, 1$ is due to the fact that there the correlations are exactly zero ranged. This, how-

ever, is not the case for intermediate τ , especially near the QPT, so how S_{top} works as an order parameter, and how sharply its derivative detects the QPT, are rather nontrivial.

In the presence of the perturbation $h^x(j)$, which tends to destroy the loop structure, S_{top} detects the TOQPT up to the value $P \sim 25$, after which a transition occurs: see Fig. 7 (inset). Overall, Figs. 6 and 7 show that the robustness of TO against perturbations is a feature of the whole topological phase and not only of the analytically solvable model at $\tau=1$. Finally, we note another remarkable fact: setting the x perturbation V to zero, and moving backward in time from $\tau=1$, we can view also the tension term H_ξ as a perturbation. This is due to the fact that the toric code is symmetric under the exchange $x \leftrightarrow z$ in the spin components. The flatness of S_{top} in Fig. 6 (squares and circles) shows the robustness of the topological phase against this perturbation (see also Ref. 7).

VII. CONCLUSIONS

We have presented a comprehensive numerical study of a TOQPT. Our results show, using a variety of previously proposed QPT detectors, that this is a second order transition. Unlike the other detectors, the topological entropy S_{top} is capable of distinguishing this TOPQT from a standard one, already for small lattices. Strikingly, the model and its TOQPT are highly robust against random perturbations not only deep inside the topological phase, where the gap protects the ground state from perturbations, but—even more surprisingly—at the gapless critical point. This phenomenon requires further investigation to be properly understood. Moreover, S_{top} detects the TOQPT for perturbations of strength up to 20% of the strongest couplings. Of course finite-size effects can be important, but it is not possible at present to compute S_{top} exactly without direct diagonalization, and this poses limits on the maximum size of systems that can be studied.

ACKNOWLEDGMENTS

We acknowledge financial support by DOE, Grant No. DE-FG02-05ER46240 (to S.H.), and by NSF Grants No. CCF-0523675 and No. CCF-0726439, and ARO-QA Grant No. W911NF-05-1-0440 (to D.A.L.). Computational facilities have been generously provided by the HPCC-USC Center.

¹S. Sachdev, *Quantum Phase Transitions* (Cambridge University Press, Cambridge, England, 2001).

²X. G. Wen, Phys. Rev. B **40**, 7387 (1989); Int. J. Mod. Phys. B **4**, 239 (1990); Adv. Phys. **44**, 405 (1995); *Quantum Field Theory of Many-Body Systems* (Oxford, New York, 2004).

³X.-G. Wen and Q. Niu, Phys. Rev. B **41**, 9377 (1990).

⁴A. Y. Kitaev, Ann. Phys. **303**, 2 (2003).

⁵M. H. Freedman *et al.*, Bull., New Ser., Am. Math. Soc. **40**, 31 (2003).

⁶A. Hamma and D. A. Lidar, Phys. Rev. Lett. **100**, 030502 (2008).

⁷S. Trebst, P. Werner, M. Troyer, K. Shtengel, and C. Nayak,

Phys. Rev. Lett. **98**, 070602 (2007).

⁸T. J. Osborne and M. A. Nielsen, Phys. Rev. A **66**, 032110 (2002); A. Osterloh *et al.*, Nature (London) **416**, 608 (2002); J. Vidal, G. Palacios, and R. Mosseri, Phys. Rev. A **69**, 022107 (2004); G. Vidal, J. I. Latorre, E. Rico, and A. Kitaev, Phys. Rev. Lett. **90**, 227902 (2003).

⁹L.-A. Wu, M. S. Sarandy, and D. A. Lidar, Phys. Rev. Lett. **93**, 250404 (2004); L. A. Wu, M. S. Sarandy, D. A. Lidar, and L. J. Sham, Phys. Rev. A **74**, 052335 (2006).

¹⁰P. Zanardi and N. Paunković, Phys. Rev. E **74**, 031123 (2006).

¹¹A. Kitaev and J. Preskill, Phys. Rev. Lett. **96**, 110404 (2006); M. Levin and X.-G. Wen, *ibid.* **96**, 110405 (2006).

- ¹²A. Hamma, P. Zanardi, and X.-G. Wen, *Phys. Rev. B* **72**, 035307 (2005).
- ¹³A. Hamma, R. Ionicioiu, and P. Zanardi, *Phys. Lett. A* **337**, 22 (2005).
- ¹⁴A. Hamma, R. Ionicioiu, and P. Zanardi, *Phys. Rev. A* **71**, 022315 (2005).
- ¹⁵W. H. Press *et al.*, *Numerical Recipes* (Cambridge University Press, Cambridge, England, 1992), pp. 462–469.
- ¹⁶E. R. Gagliano, E. Dagotto, A. Moreo, and F. C. Alcaraz, *Phys. Rev. B* **34**, 1677 (1986).
- ¹⁷S. Elitzur, *Phys. Rev. D* **12**, 3978 (1975).
- ¹⁸C. Castelnovo and C. Chamon, *Phys. Rev. B* **77**, 054433 (2008).
- ¹⁹H. T. Quan, Z. Song, X. F. Liu, P. Zanardi, and C. P. Sun, *Phys. Rev. Lett.* **96**, 140604 (2006).
- ²⁰L. Campos Venuti and P. Zanardi, *Phys. Rev. Lett.* **99**, 095701 (2007).
- ²¹D. Beckman, D. Gottesman, A. Kitaev, and J. Preskill, *Phys. Rev. D* **65**, 065022 (2002).